Published in final edited form as:
Gene Expr Patterns. 2014 November ; 16(2): 104–113. doi:10.1016/j.gep.2014.11.001.

Temporal and Spatial Expression of Tight Junction Genes During Zebrafish Pronephros Development

Robert McKee[1,2], **Gary F. Gerlach**[1,2], **Jonathan Jou**[1], **Christina N. Cheng**[1], and **Rebecca A. Wingert**[1,3]

[1]Department of Biological Sciences and Center for Zebrafish Research, University of Notre Dame, Notre Dame, IN 46556, USA

Abstract

The kidney is comprised of nephrons—epithelial tubes with specialized segments that reabsorb and secrete solutes, perform osmoregulation, and produce urine. Different nephron segments exhibit unique combinations of ion channels, transporter proteins, and cell junction proteins that govern permeability between neighboring cells. The zebrafish pronephros is a valuable model to study the mechanisms of vertebrate nephrogenesis, but many basic features of segment gene expression in renal progenitors and mature nephrons have not been characterized. Here, we analyzed the temporal and spatial expression pattern of tight junction components during zebrafish kidney ontogeny. During nephrogenesis, renal progenitors show discrete expression domains of *claudin (cldn) 15a, cldn8, occludin (ocln) a, oclnb, tight junction protein (tjp) 2a, tjp2b*, and *tjp3*. Interestingly, transcripts encoding these genes exhibit dynamic spatiotemporal domains during the time when pronephros segment domains are established. These data provide a useful gene expression map of cell junction components during zebrafish nephrogenesis. As such, this information complements the existing molecular map of nephron segment characteristics, and can be used to characterize kidney development mutants as well as various disease models, in addition to aiding in the elucidation of mechanisms governing epithelial regeneration after acute nephron injury.

Keywords

kidney; nephron; pronephros; zebrafish; tight junction protein; claudin; occludin; nephrogenesis; renal progenitor; proximal tubule; distal tubule

[3]Correspondence to: Rebecca A. Wingert, Ph.D., Department of Biological Sciences, 100 Galvin Life Sciences Building, University of Notre Dame, Notre Dame, IN 46556-5688. Phone: (574)-631-0907. Fax: (574)-631-7413. rwingert@nd.edu.
[2]Co-first author, equal contributions

INTRODUCTION

The kidney is comprised of specialized epithelial tubules termed nephrons that perform important homeostatic tasks including, but not limited to, the reabsorption of nutrients, water balance, and urine production. Vertebrate nephrons are commonly made up of three different functional parts: a blood filter, tubule, and duct (Saxen, 1987; Reimschuessel, 2001). The filter is specialized to collect plasma from the blood, which is then funneled into the tubule (Kroeger and Wingert, 2014). The nephron tubule is regionalized into a series of proximal and distal segments that accomplish the discrete and complex tasks of modifying the filtrate to recover or secrete macromolecules ranging from metabolites to electrolytes (Cheng and Wingert, 2014). The different tubule segments exhibit unique combinations of ion channels and transporter proteins, allowing them to facilitate the intracellular uptake and secretion of solutes (Reilly, et al., 2007). Additionally, the success of the kidney is contingent on the ability of the nephron tubule to control and block the paracellular movement of molecules, enabling the precise regulation and containment of nephron contents (Denker and Sabath, 2011). Nephron cells are thus also characterized by the components of these specialized cell-to-cell junctions. Furthermore, the important functions of these factors in renal physiology are emphasized by the association between various chronic renal disease conditions and abnormal epithelial cell junction formation (Balkovetz, 2009; Hou, et al., 2013).

The zebrafish pronephros, or embryonic kidney, is a useful model to study nephron biology because it contains nephrons that have a conserved structure with those of other vertebrates, such as amphibians and mammals (Wingert and Davidson, 2008). Studies of zebrafish nephron segment patterning, morphogenesis, and physiology have emerged as powerful research areas that are applicable to human nephrology (Ebarasi, et al., 2011; Gerlach and Wingert, 2013). During zebrafish pronephros formation, bilateral stripes of renal progenitors emerge from the intermediate mesoderm (IM) (Drummond, et al., 1998). Over the first day of development, these renal progenitors undergo patterning events that fashion them into parallel nephrons (refer to Figure 6) (Wingert, et al., 2007), and undergo a mesenchymal to epithelial transition (MET) to become epithelial tubules (Gerlach and Wingert, 2014). The nephrons join rostrally to form a common blood filter (also known as a glomerulus), comprised of renal podocyte (P) cells and a capillary tuft, that is connected to tubules comprised of the following segments: neck (N), proximal convoluted and straight tubules (PCT, PST), corpuscles of Stannius (CS), and the distal early and late (DE, DL) tubules (Wingert, et al., 2007). The nephrons drain into pronephric ducts (PD) that fuse caudally at the cloaca (C), where waste is finally excreted (Wingert, et al., 2007). During pronephric development, the renal progenitors undergo highly dynamic alterations in the spatiotemporal expression domains of transcription factors, leading to the emergence of the aforementioned segments (Serluca and Fishman, 2001; Wingert, et al., 2007; Wingert and Davidson, 2011; Li, et al., 2014). Comparative analysis of solute gene expression profiles among zebrafish, amphibian, mouse, and human nephrons has demonstrated that segment characteristics are well conserved across these vertebrate species (Wingert and Davidson, 2008).

To date, the characterization of gene expression domains in the zebrafish pronephric kidney segments has been largely limited to transcription factors during nephron patterning and

solute transporters at the time points when discrete nephron segments have formed (Wingert, et al., 2007; Wingert and Davidson, 2011; O'Brien, et al., 2011; Marra and Wingert, 2014; Miceli, et al., 2014; Naylor, et al., 2014; Li, et al., 2014). However, vertebrate nephron functionality is crucially contingent on the aforementioned cell-cell interactions that create tight or leaky attachments between adjacent epithelial cells (Balkovetz, 2006; Denker and Sabath, 2011). This permeability between neighboring nephron cells is governed by interactions between specific proteins that comprise their tight junctions (Balkovetz, 2006; Denker and Sabath, 2011). Annotating the regional differences in tight junction gene expression is integral to understanding the molecular characteristics of the zebrafish kidney, and ultimately its physiology.

Tight junctions are located near the apical surface and consist of a cytoplasmic plaque of proteins as well as intracellular protein fibers (Gonzalez-Mariscal, et al., 2007; Cereijido, et al., 2008). Across vertebrate tissues, the expression of discrete tight junction components establishes unique properties for various cell types. The cytoplasmic plaque contains the tight junction proteins (TJ; also known as zona occludens (ZO)), which function to link the complex with the cytoskeletal network. Additional proteins found in these junctions include the Occludins (Ocln), a family of tetraspan membrane proteins, and the Claudins (Cldn), a second distinct family of tetraspan membrane proteins. Ocln proteins, which have been found to be non-essential for the formation of tight junctions, influence paracellular permeability by increasing trans-epithelial resistance (TER) between adjacent cells. Cldns, on the other hand, are essential for tight junction formation, and are primarily responsible for regulating the paracelluallar permeability properties of epithelia. Generally, vertebrates possess over 20 Cldn gene family members (Hewitt, et al., 2006; Günzel and Fromm, 2012), and these have been greatly increased in the genomes of teleost fishes, where some species possess over 50 Cldn genes (Kolosov, et al., 2013). The barrier function that these two protein families contribute to the kidney is essential for its function, and several renal diseases have been associated with mutations in their members (Balkovetz, 2009). Another critical role that tight junctions perform is the maintenance of cell polarity through a so-called fence function, in which they prohibit apical protein complexes from diffusing into the basolateral region and vice versa (Gonzalez-Mariscal, et al., 2007; Cereijido, et al., 2008). Through their links to the cytoskeleton, junctional complexes help to regulate its organization and functional activities (Fanning, et al., 2011). Further, epithelial cell function is modulated by signaling pathways that phosphorylate various tight junction components, situating the tight junction as an assemblage of dynamic elements that significantly influence cell phenotype in both health and disease states (Gonzalez-Mariscal, et al., 2008).

Interestingly, genes encoding intercellular junctional proteins, such as Cldns, are known to be regionally expressed in the mammalian kidney, such that TER is increased along the proximo-distal length of each nephron (Denker and Sabath, 2011). Whether zebrafish nephrons exhibit analogous regional expression patterns of tight junction genes has not yet been established. Since the simple embryonic kidney of the zebrafish is an advantageous model for nephrology research, it is important to delineate tight junction expression across renal cell types. Previous work by Kiener, et al., (2007) has documented the expression pattern of several *tjp* genes throughout tissues of the whole zebrafish embryo during

ontogeny. However, sparse information was gathered regarding the expression of these genes within the pronephros, and other tight junction components were not examined. In this study, we performed a detailed analysis of the transcript localization of these *tjp* genes and other junctional components in the developing zebrafish pronephros using whole mount *in situ* hybridization (WISH). We found that zebrafish renal progenitors exhibit dynamic alterations in tight junction gene expression. Furthermore, tight junction genes show an overlapping, nested arrangement in developing nephrons, such that distal nephron regions express the greatest number of factors. With these data, we have thus characterized a spatiotemporal map of zebrafish *tjp, ocln*, and *cldn* gene expression domains during nephrogenesis. Overall, these findings provide a useful addition to the current catalogue of nephron segment characteristics in the zebrafish and can be used to further the understanding of renal physiology.

1. RESULTS

1.1 Overview of tight junction genes and pronephros expression analysis

Vertebrate nephrons are characterized by the regional expression of tight junction components which enables relatively leaky proximal tubule segments to reabsorb solutes readily, while distal tubule segments tightly regulate solute movement in order to fine-tune salt and electrolyte levels in the body (Denker and Sabath, 2011). Regional and/or graded expression of Cldn and Occludin genes typifies mammalian nephrons (Denker and Sabath, 2011). Interestingly, previous gene expression analysis has demonstrated that at two *tjp* genes, *tjp2a* and *tjp3*, are expressed in the distal pronephros (Kiener, et al., 2007).

To examine whether zebrafish nephrons exhibit a conserved regional distribution of tight junction genes during nephrogenesis, we performed time course studies to examine the expression domains of these genes as well as other tight junction genes annotated in the zebrafish genome. We implemented a modified WISH method which incorporates the use of dextran sulfate to analyze the renal expression of *claudin (cldn) 15a, cldn8, occludin (ocln) a, oclnb*, and *tight junction protein (tjp) 1a, 1b, 2a, 2b*, and *3*, as described in the following sections. To precisely map each gene expression domain in the developing pronephros, we utilized a double WISH approach previously established by our lab that uses a riboprobe to label *slow myosin heavy chain 1* (*smyhc1*) to demarcate the embryonic somites located adjacent to the nephron territory (Wingert, et al., 2007; Wingert and Davidson, 2011; Li, et al., 2014). This method enables each gene expression domain to be compared to the eventual location of the various pronephric tubule and duct segments. Of note, the renal progenitors emerge from the intermediate mesoderm, and maintain a mesenchymal character until the 20–22 somite stage (ss), at which time they undergo MET, thereby forming tubules (Gerlach and Wingert, 2014). By the 28 ss (approximately 1 day post fertilization (dpf)), discrete segment boundaries are defined based on an expression signature that consists of numerous solute transporter genes (Wingert, et al., 2007). At the 28 ss, the nephron segments occupy the following positions: the neck is located adjacent to somite 4, the PCT is located adjacent to somites 5–8, the PST is located next to somites 9–11, the DE is located next to somites 12–13, the DL and PD share partially overlapping domains located at somites 15–18, the CS

is located at somite 15, and the C is located at somite 18 (refer to Figure 6) (Wingert, et al., 2007).

1.2 Expression of *tjp* transcripts during nephrogenesis

First, we analyzed the expression of *tjp* gene transcripts using WISH at the 16, 18, 20, 22, 26, and 28 ss as well as the 36 and 48 hours post fertilization (hpf) time points, and found that *tjp2a, tjp2b* and *tjp3* were all expressed in the pronephros (Figure 1, Table S1, Figure S1). Expression of *tjp1a* and *tjp1b* was not localized to the renal progenitors or pronephros at any of these developmental stages (data not shown). In contrast, transcripts encoding *tjp2a* were first present in the IM at the 18 ss, with expression confined to renal progenitors located adjacent to somites 9–18 (Figure 1). Expression of *tjp2a* was maintained in this region through the 22 ss, and then showed an expanded domain at the 26 ss, when the entire length of the nephron tubule expressed this transcript (Figure 1). By the 28 ss, the expression of *tjp2a* was reduced in the proximal tubule, in the region located adjacent to somites 4–11, while the distal tubule maintained expression in the region adjacent to somites 12–18 (Figure 1). By 36 hpf, the *tjp2a* transcript was only detected in the distal regions of the pronephros, and the intensity was reduced greatly by 48 hpf (Figure 1).

Analysis of *tjp2b* transcripts in the developing pronephros revealed a dynamic expression pattern similar to the pattern of *tjp2a* expression. *tjp2b* was first detected at the 18 ss in renal progenitors located adjacent to somites 9–18 (Figure 1). The *tjp2b* expression domain expanded at the 20 ss, with transcripts detected in the entire length of the renal progenitor field, and was maintained between the 22–28 ss when tubulogenesis has occurred (Figure 1). At 36 hpf, *tjp2b* transcripts were weakly expressed in the distal tubule and PD, but by 48 hpf, low levels of *tjp2b* transcripts were detected throughout the pronephros (Figure 1).

In contrast to *tjp2a* and *tjp2b*, transcripts encoding *tjp3* exhibited strong expression as early as the 16 ss, with expression occurring throughout the entire developing pronephros (Figure 1). *tjp3* transcripts were highly expressed in the distal renal progenitors starting at somite 12 through to the terminus of the yolk sac extension, and were weakly expressed in the renal progenitors located next to somites 4–12 (Figure 1). Proximal expression of the *tjp3* transcript increased in intensity between 18–22 ss, such that strong levels were detected along the entire pronephros tubule by the 22 ss (Figure 1). Commensurate expression continued throughout the tubule with a reduction in intensity occurring post 28 somites, and a reduction to the distal regions of the pronephros occurred by 36 and 48 hpf (Figure 1).

1.3 Expression of *ocln* transcripts during nephrogenesis

Next, we investigated the expression patterns of two occludins, *occludin a* (*oclna*) and *occludin b* (*oclnb*). The presence of these genes in the pronephros has been annotated at the 19–25 ss (Thisse and Thisse, 2004), but prior and subsequent time points were not reported. Thus, we examined the spatial domains of these transcripts in the developing pronephros between the 5 ss through 36 hpf stages (Figure 2, data not shown). Renal expression of both *ocln* transcripts was first detected in a small region of cells at the caudal-most region of the yolk sac extension at 16–18 ss (Figure 2). By the 20 ss, *oclna* transcripts were present throughout the renal progenitors located adjacent to somites 4–18, with the strongest

intensity in cells located in the DL and PD regions adjacent to somites 17–18 (Figure 2). By the 22 ss, proximal expression of *oclna* began to diminish, while expression in the distal regions remained strong (Figure 2). By the 28 ss, expression was absent from all regions of the pronephros except the DL, where faint expression levels were detected, and the PD and cloacal regions where strong levels were observed (Figure 2). By 36 hpf, *oclna* transcript was absent from the pronephros tubule and confined to the terminus of the PD where the cloaca is located (Figure 2).

The *oclnb* transcript first appeared at the 20 ss as well; however, its expression never expanded outside of the distal-most regions of the renal progenitor fields and the subsequent pronephros tubules (Figure 2). Even so, *oclnb* did exhibit stronger DL and PD expression at the 22 ss until the 28 ss, with high levels of transcripts detected adjacent to somites 14–18 (Figure 2). Similar to the other tight junction gene transcripts examined, *oclnb* was down regulated after the 28 ss with only very weak expression occurring by 36 hpf (Figure 2).

1.4 Expression of *cldn* transcripts during nephrogenesis

In mammals, the expression domains of Cldns 1–4, Cldns 6–11, and Cldns 14–16, are restricted to one or several nephron segments (Denker and Sabath, 2011). To determine whether this gene signature is conserved in zebrafish, we surveyed the literature and the Zebrafish Information Network database for the existence of zebrafish orthologues. From this we found that cDNA clones were available for zebrafish *cldn1, 2, 7, 8, 10, 11, 15a* and *15b* (Kollmar, et al., 2001). WISH was performed using antisense riboprobes to examine whether this particular panel of *cldn* genes was expressed in the zebrafish pronephros between the 24–28 ss (data not shown). Of these, only transcripts encoding *cldn15a* and *cldn8* were observed in the nephron. Thus, we proceeded to further characterize the temporal and spatial dynamics of these two *cldn* genes during nephrogenesis.

Interrogation of the *cldn15a* and *cldn8* transcripts revealed a dynamic, overlapping expression pattern during the course of pronephros formation (Figures 3–5). *cldn15a* was strongly expressed in renal progenitors at the 16 ss throughout the proximal region, in a domain adjacent to somites 4–8, and was expressed at low levels in renal progenitors adjacent to somites 9–11, which is where the PST will eventually emerge (Figure 3). Additionally, *cldn15a* transcripts were expressed in the primitive blood islands that constitute an intermediate cell mass (ICM) (Wingert and Zon, 2006) at 16 ss and until 22 ss, which can be distinguished from the renal progenitors because they are situated at the midline (see dorsal views, Figure 3). By the 24–26 ss, *cldn15a* transcripts were maintained in the proximal regions adjacent to somites 4–11, with higher levels in the domain adjacent to somites 4–8 (Figure 3). After the 26 ss, a reduction in the presence of *cldn15a* transcripts was seen in the proximal pronephros, but was nonetheless maintained (Figure 3). At 36 and 48 hpf, *cldn15a* transcripts in the proximal tubule were distinguished from the concomitant expression of this gene throughout the gastrointestinal tract (Figure 3).

As seen with *cldn15a*, transcripts encoding *cldn8* were present in renal progenitors at the 16 ss but were localized to the distal regions of the developing pronephros (Figure 4). Furthermore, *cldn8* transcripts were found in renal progenitors located adjacent to somites 9–18 (Figure 4). Between 18–22 ss, the intensity of *cldn8* expression increased in renal

progenitors located adjacent to somites 12–18, where the distal segments (DE, DL, PD) later emerge (Figure 4). By the 24–26 ss, there was a subsequent decrease of *cldn8* expression in renal cells located next to somites 9–12, such that intense *cldn8* expression was ultimately localized to the DL-PD segments located between somites 14–18 at this time (Figure 4). At 36 and 48 hpf, *cldn8* expression was maintained in the DL-PD (Figure 4).

Due to the strong expression of *cldn15a* and *cldn8* at the 16 ss stage, we next sought to elucidate the onset of *cldn* expression in the renal progenitors, and therefore examined developmental stages ranging from the 5–16 ss (Figure 5, data not shown). Interestingly, *cldn15a* transcripts were present at the 5 ss in renal progenitors, and the expression of this gene spread in both proximal and distal directions by the 12–13 ss, and increased in intensity as well (Figure 5). Further, we noted that *cldn15a* transcripts were present in primitive blood ICM precursors at the 12–13 ss, which are situated in parallel stripes adjacent to the renal progenitors, but in a more medial location (Figure 5). Finally, *cldn8* transcripts were detected in renal progenitors as early as the 12–13 ss in a distal domain located adjacent to somite 9 that extended down the length of the IM field in the embryonic tailbud (Figure 5).

3. DISCUSSION

Here, we have expanded the knowledge of kidney development in the zebrafish embryo by annotating the temporal and spatial expression domains of tight junction components during the process of nephrogenesis. This expression profiling provides useful new insights into the dynamic transcriptional profile of cells within the developing nephron, revealing that tight junction genes are expressed in a series of overlapping domains along the nephron length (Figure 6), and add substantial new insights to the initial observations of these genes in the renal progenitors (Thisse and Thisse, 2004; Kiener, et al., 2007). This thorough temporal and spatial map of tight junction gene expression patterns provides both a necessary and important foundation for further study of epithelial cell junction assembly and regulation during zebrafish pronephros development. The expression data compiled in this study provides information relevant to not just to future nephrogenesis studies, but can be utilized to study epithelial changes associated with kidney injury, regeneration, and models of renal diseases like polycystic kidney disease (PKD) in zebrafish.

3.1 Overlapping, nested domains of tight junction genes and their spatiotemporal dynamics

Nephrons have intricate physiological roles in homeostasis, fulfilling the tasks of filtering the blood, modifying the filtrate to reabsorb nutrients and maintain osmoregularity, and finally excreting the metabolic waste. To precisely conduct and balance these functions, cells within the nephron must control the ability of specific molecules and ions to move from the filtrate back into the body (Balkovetz, 2009). This is accomplished by the differential expression of specific intracellular transport proteins in various regions of the nephron and proper expression and assembly of junctional complexes that govern paracellular permeability (Balkovetz, 2009).

In the present study, we have identified an overlapping, nested arrangement of tight junction gene expression domains during zebrafish pronephros formation. For example, during the

26–28 ss (which corresponds to approximately 1 dpf), transcripts encoding *tjp2a*, *tjp2b*, and *tjp3* are expressed throughout the nephrons, while *cldn15a* and *cldn8* are restricted to respective proximal and distal domains (Figure 6). At this time, the domains of the DL segment, PD, and C show specific expression of *oclna* and *oclnb* (Figure 6), with the highest transcript levels within the PD and C regions (Figure 2). These observations indicate that segment regional identities along the zebrafish nephron are associated with particular cell junction transcription signatures. Mammalian nephrons similarly possess regionalized cell junction expression along their proximo-distal length, with the expression of various Cldn genes being perhaps the best characterized to date (Denker and Sabath, 2011). The conserved pattern of solute transporter domains across nephron segments has been recognized among vertebrates, including zebrafish, frogs, and mammals (Wingert and Davidson, 2008). The data presented in the current study adds to this understanding by contributing the new insight that the expression of cell junction components varies regionally across the nephron segments in the zebrafish, illustrating another similarity among higher vertebrates. One interesting example of conservation is the pattern of Cldn8 across vertebrate species. In the mouse nephron Cldn8 is restricted to the PST, distal tubule and collecting duct (Kiuchi-Saishin, et al., 2002; Li, et al., 2004), while in the human nephron Cldn8 has been colocalized thus far with distal markers (Kirk, et al., 2010). Here, we discovered that the zebrafish orthologue, *cldn8*, is expressed in the PST and across the distal pronephros segments and duct (Figure 4). Future studies examining the expression analysis of other zebrafish *cldn* genes, for instance, can be performed to further characterize the segmental signature of tight junction components between fish and mammals.

Additionally, through this study we uncovered several unknown aspects of *tjp* expression in the pronephros. Previous research from Kiener, et al. (2007) provided a broad tissue analysis of *tjp* genes during early zebrafish embryogenesis in which they noted the expression of *tjp2a* and *tjp3* in the distal pronephros at the 18 ss and 1 dpf. However, the extent of the *tjp2a* and *tjp3* pronephric expression domains was not scrutinized, and analysis of renal tubules at additional developmental time points was not reported. Our examinations provide a detailed spatiotemporal characterization of these genes and reveal for the first time that *tjp2b* is concomitantly and robustly expressed during pronephros formation. Deviation in expression patterns between these studies is likely due to different probes being employed in the WISH process (Figure S1). For the most part, the probes we used to detect various transcripts covered more of the mRNA sequence (Figure S1). Thus, here we were able to expand on the Kiener, et al., study (2007) by documenting the precise induction *tjp* gene expression between 16–18 ss in distal renal progenitors. Further, we show that the *tjp* genes are expressed throughout the entire tubule by 1 dpf, and that their expression becomes dramatically restricted to the PD by 2 dpf. In sum, our work documents the onset and progression of *tjp2a*, *tjp2b*, and *tjp3* expression in renal progenitors during nephrogenesis.

3.2 Functions of tight junction components during nephron development and regeneration

As these data provide a gene expression map of the tight junction transcripts present in the different nephron segments during development, they have identified genes useful for future renal development and regeneration research in zebrafish. The establishment of cell junctions is coordinated with the process of tubulogenesis in the mammalian kidney, in

which mesenchymal renal progenitors undergo a transition to an epithelial state (Little, et al., 2010). Our findings in this study reveal that the timing of tight junction expression in the zebrafish pronephros likewise correlates with the timing of MET that enables tubulogenesis, such that tight junction genes are expressed prior to lumen formation and persisting after a lumen is created at the 20–22 ss (Gerlach and Wingert, 2014). Further studies to assess the requirements of tight junction gene expression for proper tubulogenesis may provide useful insights into this process. Furthermore, after pronephros formation at 1 dpf, the nephrons undergo morphogenesis events to create a coiled PCT (Drummond, et al., 1998; Wingert, et al., 2007) that involve both distal tubule proliferation and collective cell migration (Vasilyev, et al., 2009). How cell junction components play a role in these morphogenesis events has not been characterized but may provide valuable mechanistic insights. In addition, analysis of these tight junction genes can be used to help characterize the developmental defects in genetic kidney mutants, such as those that form cysts and/or distended epithelial tubules (Drummond, et al., 1998).

Future studies assaying the expression patterns of the proteins constituting the tight junction after chemical or mechanical insult can also be used to elucidate the cellular mechanisms participating in regeneration after acute kidney injury (AKI), a condition that occurs when there is a sudden loss of renal function due to catastrophic nephron damage, typically in the tubule epithelium (Wingert and McCampbell, 2012; Li and Wingert, 2013). How the regenerated tubule epithelium is formed, including the establishment of tight junctions in these cells will be important to understand, both to appreciate *in vivo* mechanisms and to elucidate new therapeutic applications such as the emerging science of *in vitro* renal cell reprogramming (Morales and Wingert, 2014). Both the zebrafish embryonic and adult kidney are useful models for research about renal injury and regeneration (Hentschel, et al., 2005; Hellman, et al., 2010; Gerlach, et al., 2011; Johnson, et al., 2011; McCampbell et al., 2014; Zhou, et al., 2010; Diep, et al., 2011; Zhou and Hildebrandt, 2012; Huang, et al., 2013). In particular, adult zebrafish possess a high capacity for renal regeneration after AKI in the nephron tubule (Zhou, et al., 2010; Diep, et al., 2011; McCampbell and Wingert, 2014). Within just two weeks following widespread proximal tubule damage due to the nephrotoxin gentamicin, the adult kidney regenerates injured tubular epithelia and undergoes the formation of new nephrons (termed neonephrogenesis) from renal progenitors located throughout the kidney. Thus, the zebrafish provides an excellent research system in which to study both nephron regeneration and *de novo* nephron formation. The identification of genes that encode renal epithelial junctional components can be used to further characterize both of these regenerative events.

Taken together, this study has identified a cohort of genes expressed in developing renal progenitors, providing a framework for ongoing nephrogenesis studies in the zebrafish embryo, and for applications in adult nephron regeneration studies. The tractability of zebrafish for genetic studies (Lawson and Wolfe, 2011; Kroeger, et al., 2014) including chemical genetics (Poureetezadi and Wingert, 2013), in particular, makes this model especially appealing for future renal development and regeneration research. The conservation of kidney composition between fish and higher vertebrates, further demonstrated here by regionalized tight junction expression across nephron segments,

provides encouragement that zebrafish research may provide important insights about these processes in humans.

4. MATERIALS AND METHODS

4.1 Zebrafish husbandry and the staging, collection, and processing of embryos and adult kidneys

Zebrafish were maintained in the Center for Zebrafish Research at the University of Notre Dame Freimann Life Science Center. All studies were performed with approval of the Institutional Animal Care and Use Committee (IACUC), Protocol numbers 13-021 and 16-025, and under the supervision of our Veterinarian, Dr. Mark Suckow. Adult zebrafish husbandry was performed as described (Westerfield, 2007). Wild-type embryos were raised and staged as described (Kimmel, et al., 1995). Once the embryos reached the desired stage, they were dechorionated either manually (pre-18 ss) or with pronase, anesthetized with 0.2% tricaine pH 7.0, then fixed in 4% paraformaldehyde (PFA) overnight at 4°C. The next day embryos were washed twice in 1× phosphate buffered saline with 0.1% Tween-20 (Pbst) and placed in 100% methanol (MeOH) for 30 minutes at −20°C. Embryos were rehydrated with successive washes of 50% MeOH/1× Pbst, then 30% MeOH/1× Pbst, followed by two washes in Pbst. Individuals at stages older than 26 ss were bleached, rinsed with 1× Pbst, and placed in 4% PFA at room temperature for a one hour incubation. Embryos were treated with proteinase K based on their developmental stage as follows: 16–20 ss for 3 minutes; 22–28 ss for 4 minutes; 36 hpf for 5 minutes; 48 hpf for 6 minutes. Embryos were then washed twice in 1× Pbst, fixed in 4% PFA for 20 minutes at room temperature, transferred into hybridization solution (HYB+; 50% formamide, 5× SSC, 0.1% Tween-20, 5 mg/mL yeast torula RNA, 50 ug/ul heparin, 5% dextran sulfate), and stored at −20°C.

4.2 Whole mount *in situ* hybridization (WISH) of zebrafish embryos and adult kidneys

WISH was performed on fixed samples as previously described, but with the addition of dextran sulfate to hybridization solutions (Wingert, et al., 2007; Galloway, et al., 2008; Lengerke, et al., 2011; Cheng, et al., 2014). Refer to Supplemental Table 1 for gene IMAGE clones and primer sequences used to synthesize DNA templates for riboprobe production. In brief, embryos were transferred to flat-bottom microcentrifuge tubes containing 800 μL of pre-warmed HYB+ and incubated for 4 hours at 70°C. During this incubation probes were prepared by diluting RNA antisense stocks in HYB+ to 100–500 ng/500μL. Following a 4-hour incubation, the HYB+ was drawn off with a pipette and replaced with the HYB+ containing probe. The next day, the HYB+/probe was removed and samples were processed through two 30 minute 50% formamide/2× saline-sodium-citrate buffer with 0.1 Tween-20 (SSCT), a 15 minute wash in 2× SSCT, two 0.2× SSCT washes each being 30 minutes in duration, and then two 5-minute maleic acid buffer with 0.1% Tween-20 (MABT) washes. Following the MABT washes, embryos were treated with block solution for 4 hours at room temperature. The block solution was decanted and replaced with DIG antibody diluted 1:5000 in block. Samples were covered with aluminum foil to protect the antibody from light. After an overnight incubation at 4°C, embryos were taken through 10–15 MABT washes, a single wash in staining buffer and then placed in BCIP/NBT staining solution. After sufficient color development embryos were washed twice in 1× Pbst, twice for 15

minutes in 0.1 M glycine pH 2.2, then washed twice for 15 minutes in MABT. Embryos were subsequently treated with block for 30–60 minutes at room temperature, and transferred for overnight incubation at 4°C into FLUOR antibody diluted 1:5000 in block. This incubation was followed with five 15 minute MABT washes, a brief wash in staining buffer before embryos were transferred to BCIP/INT substrate solution. Again, after sufficient color development, embryos were washed twice in 1× Pbst and fixed with 4% PFA. Embryos were stored in fixative at 4°C until imaging was performed. Images were acquired with a Nikon Digital Sight DS-Fi1 on a Nikon eclipse 80i and utilizing Nikon elements software. Embryos were flat mounted as described (Cheng, et al., 2014).

Supplementary Material

Refer to Web version on PubMed Central for supplementary material.

ACKNOWLEDGEMENTS

This work was enabled through funding to RAW from the following: National Institutes of Health; Grant numbers: K01 DK083512, DP2 OD008470, R01 DK100237; March of Dimes; Grant number: Basil O'Connor Starter Scholar Award #5-FY12-75; start up funds from the University of Notre Dame College of Science and Department of Biological Sciences; gift from Elizabeth and Michael Gallagher on behalf of the Gallagher Family to the University of Notre Dame. The funders had no role in the study design, data collection and analysis, decision to publish, or preparation of the manuscript. We thank Kristen K. McCampbell for excellent lab management, and Cindy Lin for assistance with husbandry. We also thank the staffs of the Notre Dame Department of Biological Sciences and Office of Research for their support, and especially thank the Center for Zebrafish Research at Notre Dame for their outstanding dedication in the care and welfare of our zebrafish colony. Finally, we thank our research lab for their dedication, discussions, and insights about this work.

Abbreviations

cldn	*claudin*
CS	corpuscles of Stannius
DE	distal early
DL	distal late
dpf	days post fertilization
EMT	epithelial to mesenchymal transition
G	glomerulus
hpf	hours post fertilization
IM	intermediate mesoderm
myod1	*myogenic differentiation 1*
N	neck
ocln	*occludin*
P	podocyte
PCT	proximal convoluted tubule

PD	pronephric duct
PM	paraxial mesoderm
PST	proximal straight tubule
smyhc1	*slow myosin heavy chain 1*
ss	somite stage
TER	trans-epithelial resistance
tjp	*tight junction protein*
WISH	whole mount *in situ* hybridization

REFERENCES

Balkovetz DF. Claudins at the gate: determinants of renal epithelial tight junction paracellular permeability. Am. J. Physiol. Renal. Physiol. 2006; 290:F572–F579. [PubMed: 16461756]

Balkovetz DF. Tight junction claudins and the kidney in sickness and in health. Biochemica et Biophysica Acta. 2009; 1788:858–863.

Cereijido M, Contreras RG, Shoshani L, Flores-Benitez D, Larre I. Tight junction and polarity interaction in the transporting epithelial phenotype. Biochimica et Biophysica Acta. 2008; 1778:770–793. [PubMed: 18028872]

Cheng, CN.; Wingert, RA. Chapter 9: Renal system development in the zebrafish: a basic nephrogenesis model. In: Carver, E.; Lessman, C., editors. Zebrafish: Topics in Reproduction & Development. New York: Nova Scientific Publishers, New York; 2014. p. 179-214.

Cheng CN, Li Y, Marra A, Verdun V, Wingert RA. Flat mount preparation for observation and analysis of fixed zebrafish embryo specimens. J. Vis. Exp. 2014; 89:e51604.

Denker BM, Sabath E. The biology of epithelial cell tight junctions in the kidney. J. Am. Soc. Nephrol. 2011; 22:622–625. [PubMed: 21415157]

Diep CQ, Ma D, Deo RC, Holm TM, Naylor RW, Arora N, Wingert RA, Bollig F, Djordjevic G, Lichman B, Zhu H, Ikenaga T, Ono F, Englert C, Cowan CA, Hukriede NA, Handin RI, Davidson AJ. Identification of adult nephron progenitors capable of kidney regeneration in zebrafish. Nature. 2011; 470:95–100. [PubMed: 21270795]

Drummond IA, Majumdar A, Hentschel H, Elger M, Solnica-Krezel L, Schier AF, Neuhauss SC, Stemple DL, Zwartkruis F, Rangini Z, Driever W, Fishman MC. Early development of the zebrafish pronephros and analysis of mutations affecting pronephric function. Development. 1998; 125:4655–4667. [PubMed: 9806915]

Ebarasi L, Oddsson A, Hultenby K, Betsholtz C, Tryggvason K. Zebrafish: a model system for the study of vertebrate renal development, function, and pathophysiology. Curr. Opin. Nephrol. Hypertens. 2011; 20:416–424. [PubMed: 21519251]

Fanning AS, Van Itallie CM, Anderson JM. Zonula occludens-1 and -2 regulate apical cell structure and the zonula adherens cytoskeleton in polarized epithelia. Mol. Biol. Cell. 2011; 23:577–590. [PubMed: 22190737]

Galloway JL, Wingert RA, Thisse C, Thisse B, Zon LI. Combinatorial regulation of novel erythroid gene expression in zebrafish. Exp. Hematol. 2008; 36:424–432. [PubMed: 18243489]

Gerlach GF, Schrader LN, Wingert RA. Dissection of the adult zebrafish kidney. J. Vis. Exp. 2011; 54:e2839.

Gerlach GF, Wingert RA. Kidney organogenesis in the zebrafish: Insights into vertebrate nephrogenesis and regeneration. Wiley Interdiscip. Rev. Dev. Biol. 2013; 2:559–585. [PubMed: 24014448]

Gerlach GF, Wingert RA. Zebrafish pronephros tubulogenesis and epithelial identity maintenance are reliant on the polarity proteins Prkc iota & zeta. Dev Biol. 2014

Gonzalez-Mariscal L, Lechuga S, Garay E. Role of tight junctions in cell proliferation and cancer. Prog. Histochem. Cytochem. 2007; 42:1–57. [PubMed: 17502225]

Gonzalez-Mariscal L, Tapia R, Chamorro D. Crosstalk of tight junction components with signaling pathways. Biochimica et Biophysica Acta. 2008; 1778:729–756. [PubMed: 17950242]

Günzel D, Fromm M. Claudins and other tight junction proteins. Compr. Physiol. 2012; 2:1819–1852. [PubMed: 23723025]

Hellman NE, Liu Y, Merkel E, Austin C, Le Corre S, Beier DR, Sun Z, Sharma N, Yoder BK, Drummond IA. The zebrafish foxj1a transcription factor regulates cilia function in response to injury and epithelial stretch. Proc. Natl. Acad. Sci. USA. 2010; 107:18499–18504. [PubMed: 20937855]

Hentschel DM, Park KM, Cilenti L, Zervos AS, Drummond IA, Bonventre JV. Acute renal failure in zebrafish: a novel system to study a complex disease. Am. J. Physiol. Renal Physiol. 2005; 288:F923–F929. [PubMed: 15625083]

Hewitt KJ, Agarwal R, Morin PJ. The claudin gene family: expression in normal and neoplastic tissues. BMC Cancer. 2006; 6:186. [PubMed: 16836752]

Hou J, Rajagopal M, Yu ASL. Claudins and the kidney. Annu. Rev. Physiol. 2013; 75:479–501. [PubMed: 23140368]

Huang J, McKee M, Huang HD, Xiang A, Davidson AJ, Lu HA. A zebrafish model of conditional targeted podocyte ablation and regeneration. Kidney Int. 2013; 83:1193–1200. [PubMed: 23466998]

Johnson CS, Holzemer NF, Wingert RA. Laser ablation of the zebrafish pronephros to study renal epithelial regeneration. J. Vis. Exp. 2011; 54:e2839.

Keiner TK, Sleptsova-Friedrich I, Hunziker W. Identification, tissue distribution, and developmental expression of tjp1/zo-1, tjp2/zo-2, and tjp3/zo-3 in the zebrafish, Danio rerio. Gene Expr. Patterns. 2007; 7:767–776. [PubMed: 17632043]

Kimmel CB, Ballard WW, Kimmel SR, Ullmann B, Schilling TF. Stages of embryonic development of the zebrafish. Dev. Dyn. 1995; 203:253–310. [PubMed: 8589427]

Kirk A, Campbell S, Bass P, Mason J, Collins J. Differential expression of claudin tight junction proteins in the human cortical nephron. Nephrol. Dial. Transplant. 2010; 25:2107–2119. [PubMed: 20124215]

Kiuchi-Saishin Y, Gotoh S, Furuse M, Takasuga A, Tano Y, Tsukita S. Differential expression patterns of claudins, tight junction membrane proteins, in mouse nephron segments. J. Am. Soc. Nephrol. 2002; 13:875–886. [PubMed: 11912246]

Kollmar R, Nakamura SK, Kappler JA, Hudspeth AJ. Expression and phylogeny of claudins in vertebrate primordia. Proc. Natl. Acad. Sci. 2001; 98:10196–10201. [PubMed: 11517306]

Kolosov D, Bui P, Chasiotis H, Kelly SP. Claudins in teleost fishes. Tissue Barriers. 2013; 1:e25391. [PubMed: 24665402]

Kroeger PT Jr, Wingert RA. Using zebrafish to study podocyte genesis during kidney development and regeneration. Genesis. 2014; 52:771–792. [PubMed: 24920186]

Kroeger PT Jr, Poureetezadi SJ, McKee R, Jou J, Miceli R, Wingert RA. Production of haploid zebrafish embryos by in vitro fertilization. J. Vis. Exp. 2014; 89:e51708.

Lawson ND, Wolfe SA. Forward and reverse genetic approaches for the analysis of vertebrate development in the zebrafish. Dev. Cell. 2011; 21:48–64. [PubMed: 21763608]

Lengerke C, Wingert R, Beeretz M, Grauer M, Schmidt AG, Konantz M, Daley GQ, Davidson AJ. Interactions between Cdx genes and retinoic acid modulate early cardiogenesis. Dev. Biol. 2011; 163:134–142. [PubMed: 21466798]

Li W, Huey CL, Yu ASL. Expression of claudin-7 and -8 along the mouse nephron. Am. J. Physiol. Renal Physiol. 2004; 286:F1063–F1071. [PubMed: 14722018]

Li Y, Wingert RA. Regenerative medicine for the kidney: stem cell prospects and challenges. Clin. Trans. Med. 2013; 2:11.

Li Y, Cheng CN, Verdun VA, Wingert RA. Zebrafish nephrogenesis is regulated by interactions between retinoic acid, mecom, and Notch signaling. Dev. Biol. 2014; 386:111–122. [PubMed: 24309209]

Little M, Georgas K, Pennisi D, Wilkinson L. Kidney development: two tales of tubulogenesis. Curr. Top. Dev. Biol. 2010; 90:193–229. [PubMed: 20691850]

Marra A, Wingert RA. Roles of Iroquois transcription factors in kidney development. Cell Dev. Biol. 2014; 3:131.

McCampbell KK, Wingert RA. Renal stem cells: fact or science fiction? Biochem. J. 2012; 444:153–168. [PubMed: 22574774]

McCampbell KK, Wingert RA. New tides: using zebrafish to study renal regeneration. Transl. Res. 2014; 163:109–122. [PubMed: 24183931]

McCampbell KK, Springer K, Wingert RA. Analysis of nephron composition and function in the adult zebrafish kidney. J. Vis. Exp. 2014; 90:e51644. [PubMed: 25145398]

Miceli R, Kroeger PT Jr, Wingert RA. Molecular mechanisms of podocyte development revealed by zebrafish kidney research. Cell Dev. Biol. 2014; 3:138.

Morales EE, Wingert RA. Renal stem cell reprogramming: prospects for regenerative medicine. World J. Stem Cells. 2014; 6:458–466. [PubMed: 25258667]

Naylor RW, Przepiorski A, Ren Q, Yu J, Davidson AJ. HNF1β is essential for nephron segmentation during nephrogenesis. J. Am. Soc. Nephrol. 2013; 24:77–87. [PubMed: 23160512]

O'Brien LL, Grimaldi M, Kostun Z, Wingert RA, Selleck R, Davidson AJ. Wt1a, Foxc1a, and the Notch mediator Rbpj physically interact and regulate the formation of podocytes in zebrafish. Dev. Biol. 2011; 358:318–330. [PubMed: 21871448]

Poureetezadi SJ, Wingert RA. Congenital and acute kidney disease: translational research insights from zebrafish chemical genetics. General Med. 2013; 1:112.

Reilly, RF.; Bulger, RE.; Kriz, W. Structural-functional relationships in the kidney. In: Schrier, RW., editor. Diseases of the Kidney and Urinary Tract. Philadelphia: Lippincott Williams & Wilkins; 2007. p. 2-53.

Reimschuessel R. A fish model of renal regeneration and development. ILAR J. 2001; 42:285–291. [PubMed: 11581520]

Saxen, L. Organogenesis of the kidney. Cambridge: Cambridge University Press; 1987.

Serluca FC, Fishman MC. Pre-pattern in the pronephric kidney field of zebrafish. Development. 2001; 128:2233–2241. [PubMed: 11493543]

Thisse B, Thisse C. Fast Release Clones: A High Throughput Expression Analysis. Zfin Direct Date Submission. 2004http://zfin.org

Vasilyev A, Liu Y, Mudumana S, Mangos S, Lam PY, Majumdar A, Zhao J, Poon KL, Kondrychyn I, Korzh V, Drummond IA. Collective cell migration drives morphogenesis of the kidney nephron. PLoS Biol. 2009; 7:e9. [PubMed: 19127979]

Westerfield, M. The Zebrafish Book: A Guide for the Laboratory Use of Zebrafish (Danio rerio). 5th Edition. Oregon: University of Oregon Press; 2007.

Wingert, RA.; Zon, LI. Genetic dissection of hematopoiesis using the zebrafish. In: Godin, I.; Cumano, A., editors. Hematopoietic Stem Cell Development, Landes Bioscience. Georgetown, Texas: 2006. p. 18-36.

Wingert RA, Selleck R, Yu J, Song HD, Chen Z, Song A, Zhou Y, Thisse B, Thisse C, McMahon AP, Davidson AJ. The cdx genes and retinoic acid control the positioning and segmentation of the zebrafish pronephros. PLoS Genet. 2007; 3:1922–1938. [PubMed: 17953490]

Wingert RA, Davidson AJ. The zebrafish pronephros: a model to study nephron segmentation. Kid. Int. 2008; 73:1120–1127.

Wingert RA, Davidson AJ. Zebrafish nephrogenesis involves dynamic spatiotemporal expression changes in renal progenitors and essential signals from retinoic acid and *irx3b*. Dev. Dyn. 2011; 240:2011–2027. [PubMed: 21761484]

Zhou W, Boucher RC, Bollig F, Englert C, Hildebrandt F. Characterization of mesonephric development and regeneration using transgenic zebrafish. Am. J. Physiol. Renal. Physiol. 2010; 299:F1040–F1047. [PubMed: 20810610]

Zhou W, Hildebrandt F. Inducible podocyte injury and proteinuria in transgenic zebrafish. J. Am. Soc. Nephrol. 2012; 23:1039–1047. [PubMed: 22440901]

Highlights

- The zebrafish pronephros shows differential spatiotemporal expression of tjp, cldn, and ocln genes during nephrogenesis.
- Overlapping expression domains of multiple tight junction components typifies the distal tubule, while proximal tubule segments express subsets of these genes.
- Identification of tight junction components in the zebrafish pronephros provides additional tools to further study nephron formation, disease, and regeneration processes.

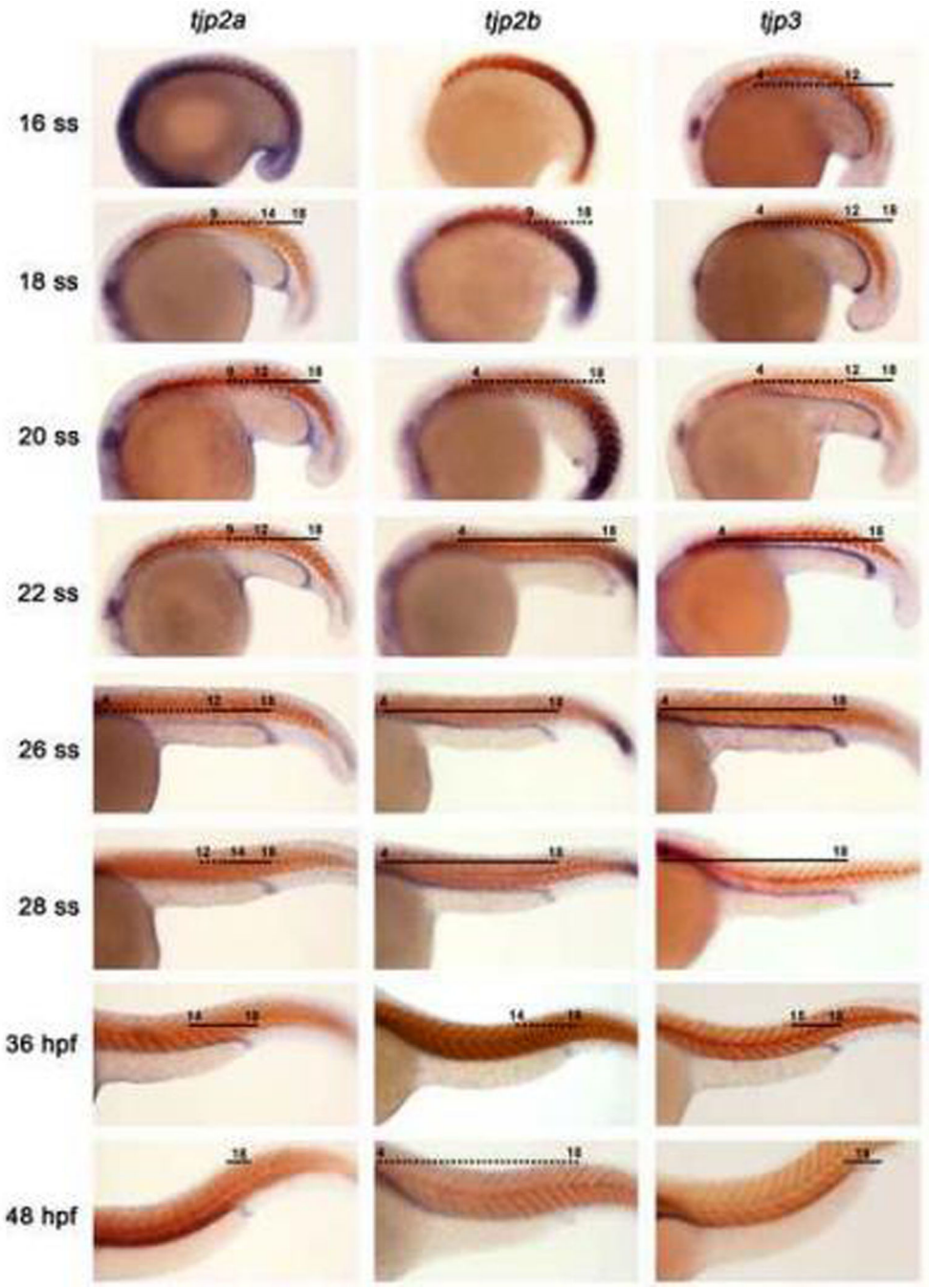

Figure 1. Expression of *tjp* transcripts during nephrogenesis

Whole mount *in situ* hybridization analysis for *tjp2a*, *tjp2b*, and *tjp3* (purple) and *smyhc1* (red) at the 16–28 somite stage (ss), 36 and 48 hours post fertilization (hpf) in wild-type embryos. Embryos are shown in lateral views with anterior to the left. Black lines (strong expression) and dotted lines (faint expression) indicated transcript domains and comparative levels, and numbers correspond to the somite position of nephron cells.

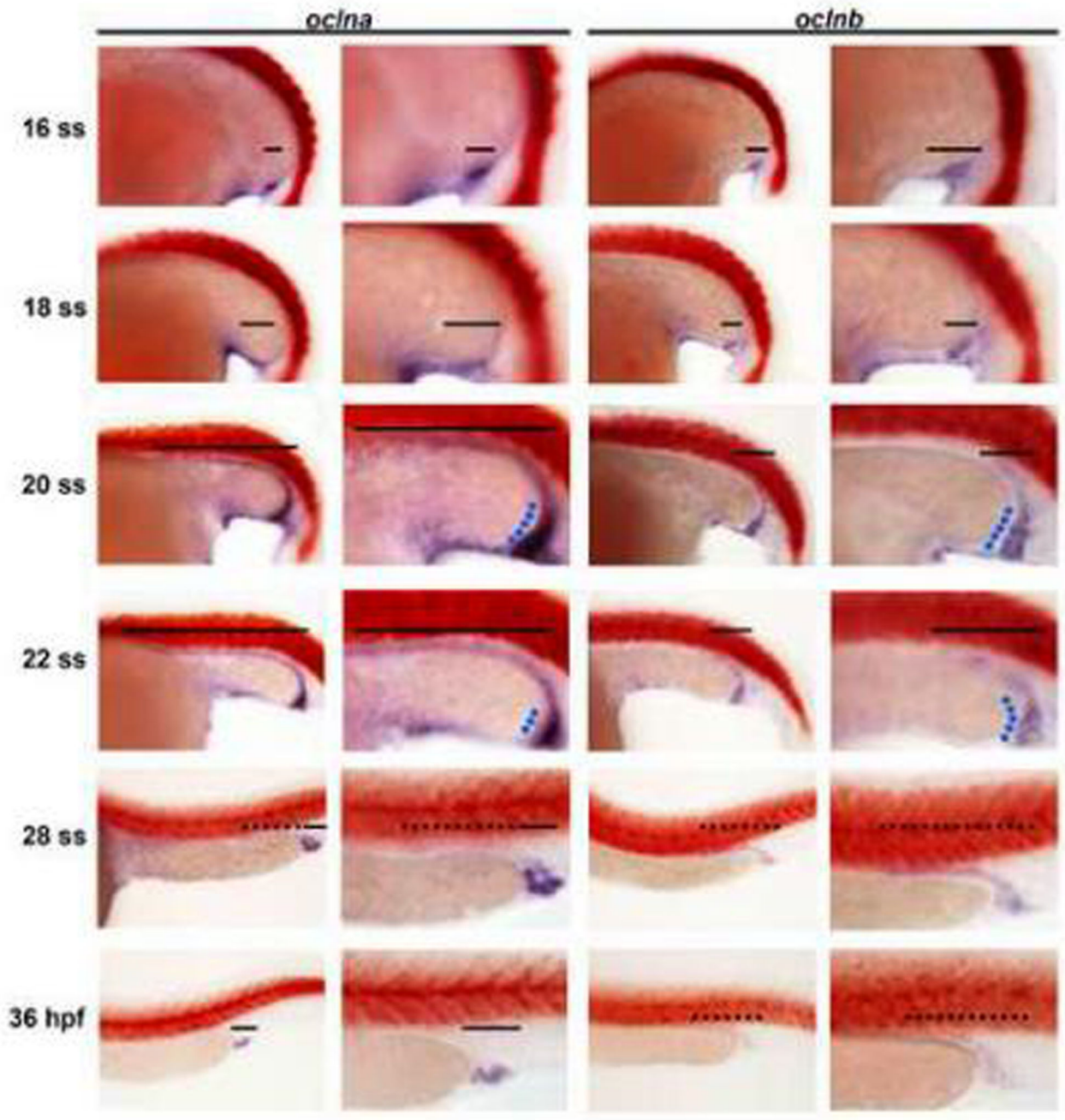

Figure 2. Expression of *ocln* transcripts during nephrogenesis

Whole mount *in situ* hybridization analysis for *oclna* and *oclnb* (purple) and *smyhc1* (red) at the 16–28 somite stage (ss), 36 and 48 hours post fertilization (hpf) in wild-type embryos. Embryos are shown in lateral views with anterior to the left. Black lines (indicating strong expression) and black dotted lines (indicating weak/low-level expression) demarcate transcript domains within the pronephros (PCT, PST, DE, DL, and PD), while blue dotted lines indicate the intense pronephros PD expression noted at particular time points.

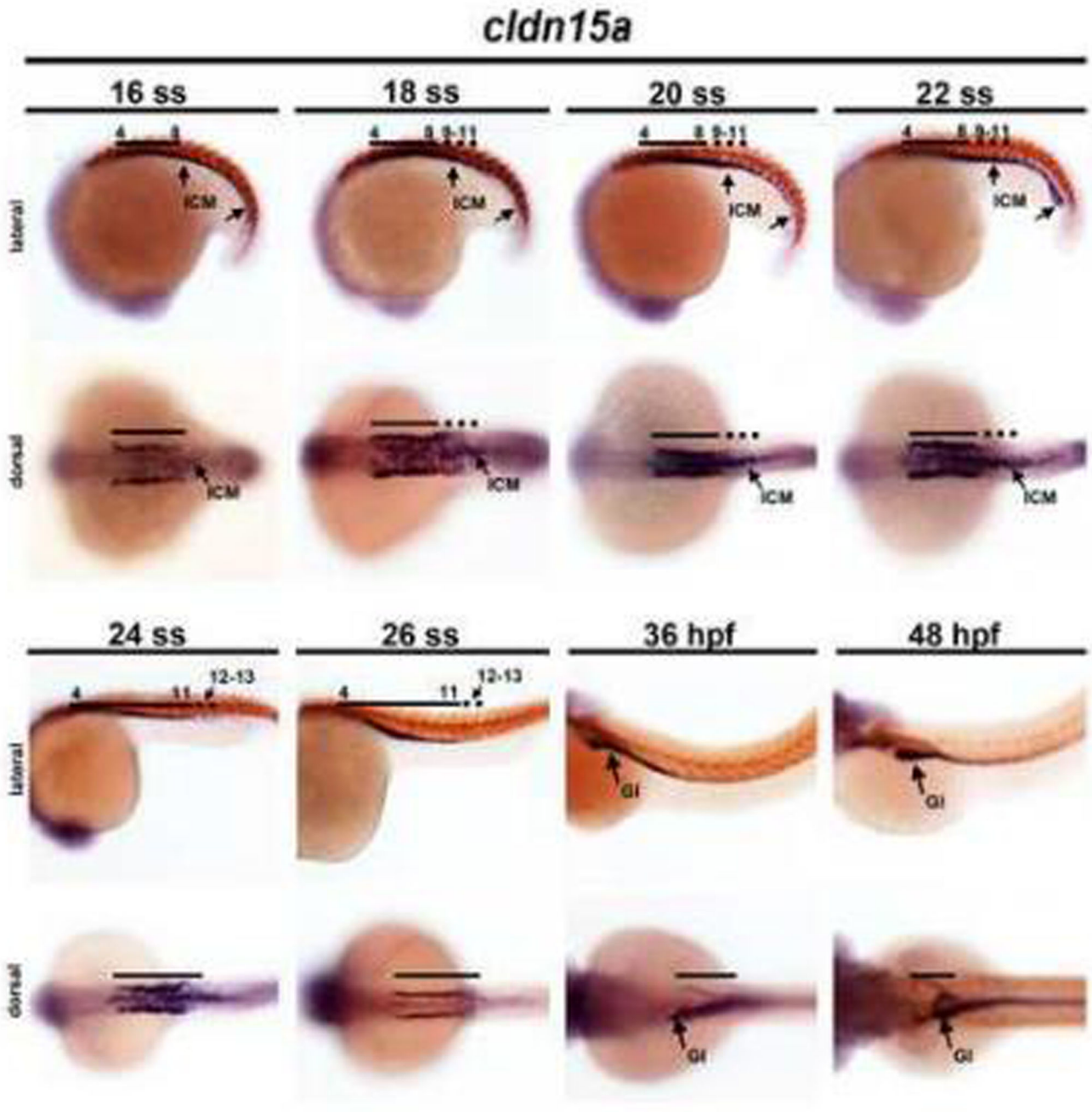

Figure 3. Expression of *cldn15a* transcripts during nephrogenesis

Whole mount *in situ* hybridization analysis for *clnd15a* (purple) and *smyhc1* (red) at the 16–28 somite stage (ss), 36 and 48 hours post fertilization (hpf) in wild-type embryos. Embryos are shown in lateral views with anterior to the left. Black lines (strong expression) and dotted lines (faint expression) indicated transcript domains and comparative levels, and numbers correspond to the somite position of nephron cells. Abbreviations: inner cell mass (ICM) denotes primitive blood, and gastrointestinal tract (GI).

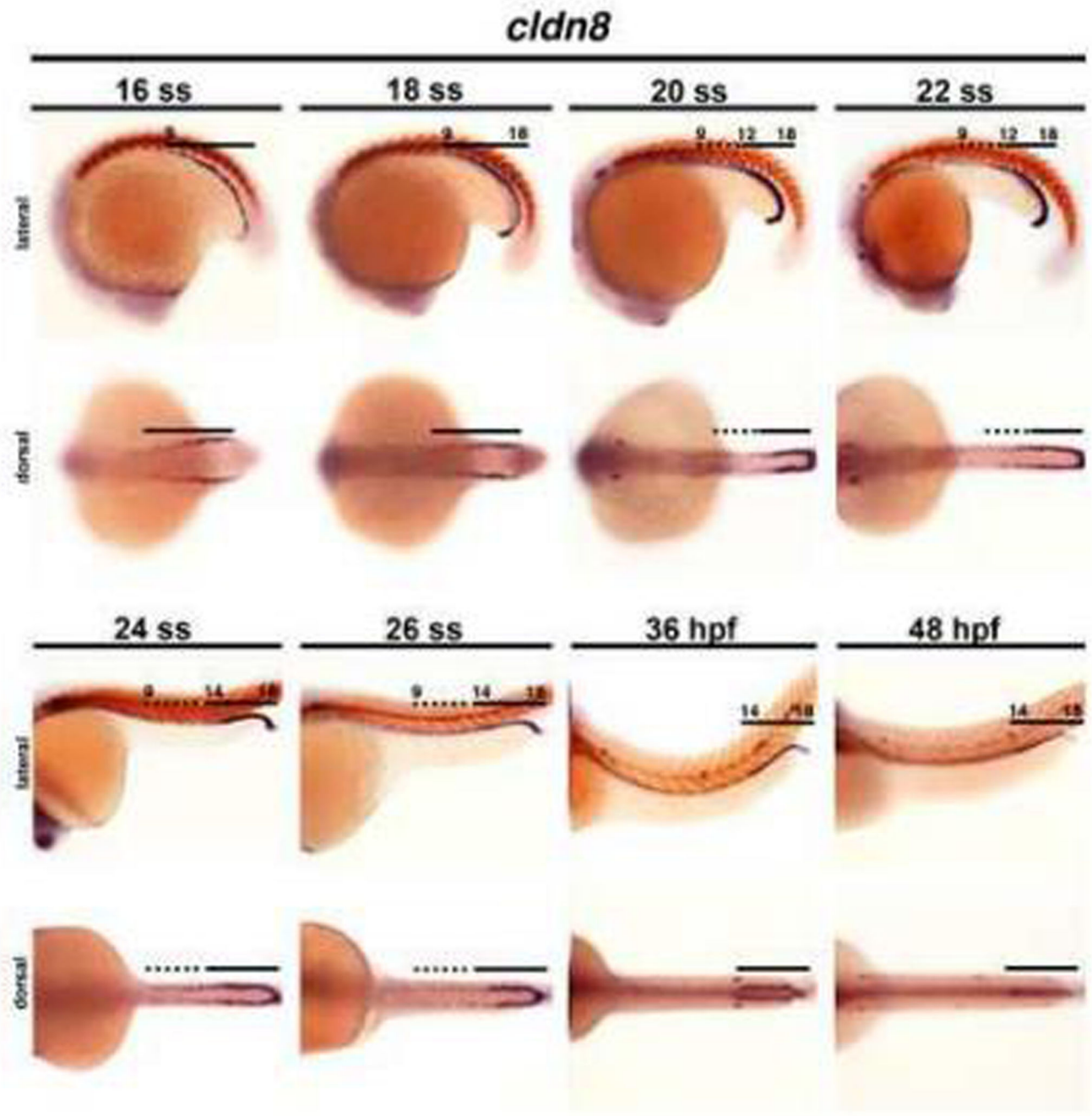

Figure 4. Expression of *cldn8* transcripts during nephrogenesis

Whole mount *in situ* hybridization analysis for *clnd8* (purple) and *smyhc1* (red) at the 16–28 somite stage (ss), 36 and 48 hours post fertilization (hpf) in wild-type embryos. Embryos are shown in lateral views with anterior to the left. Black lines (strong expression) and dotted lines (faint expression) indicated transcript domains and comparative levels, and numbers correspond to the somite position of nephron cells.

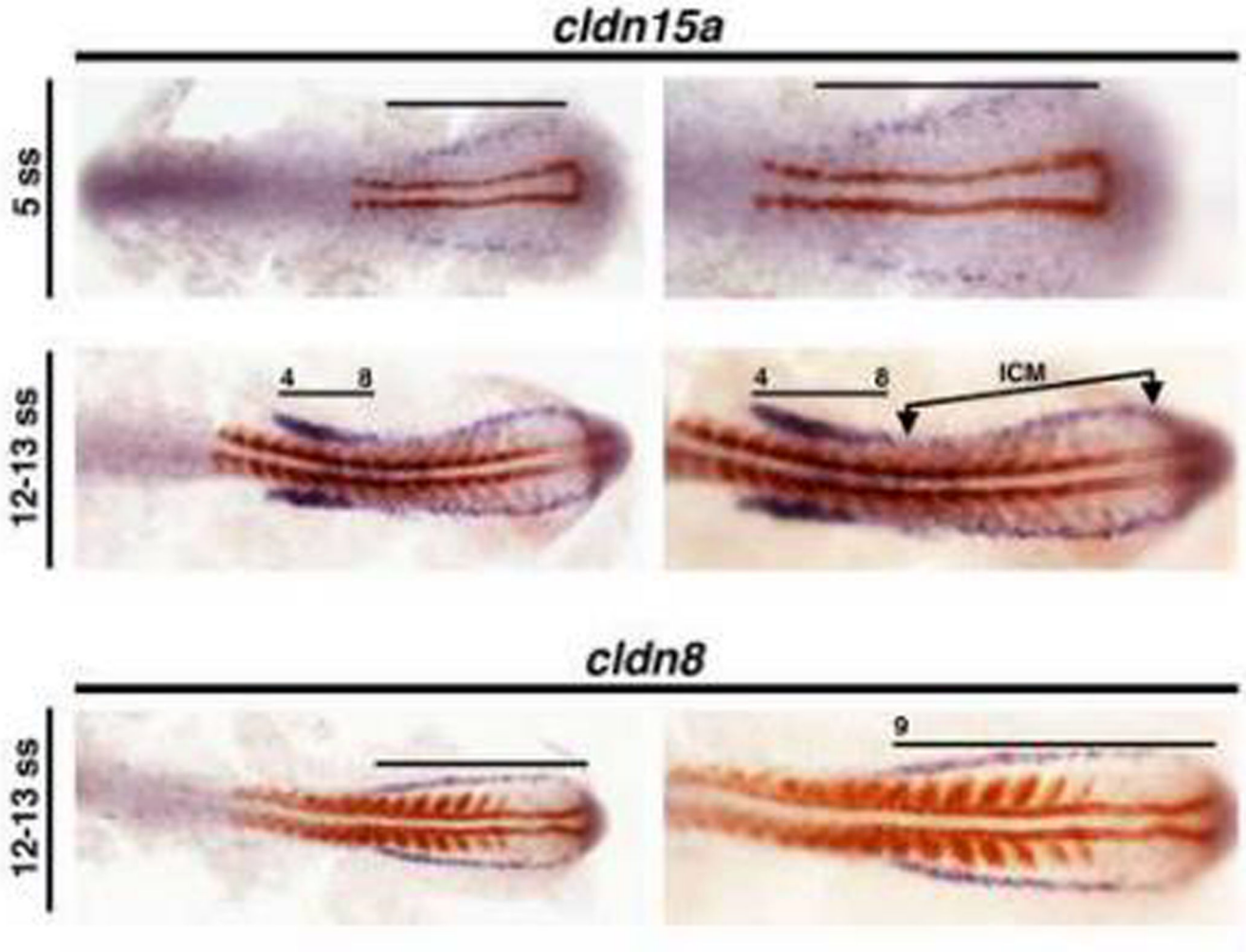

Figure 5. Renal progenitor expression domains of *cldn15a* and *cldn8*

Whole mount *in situ* hybridization analysis for *clnd15a* (purple) and *myod1* (red) at the 5–13 somite stage (ss) in wild-type embryos. Embryos are shown in dorsal view, flat-mounted, with anterior to the left. Black lines indicated transcript domains, and numbers correspond to the somite position of nephron cells. Abbreviations: inner cell mass (ICM) denotes primitive blood.

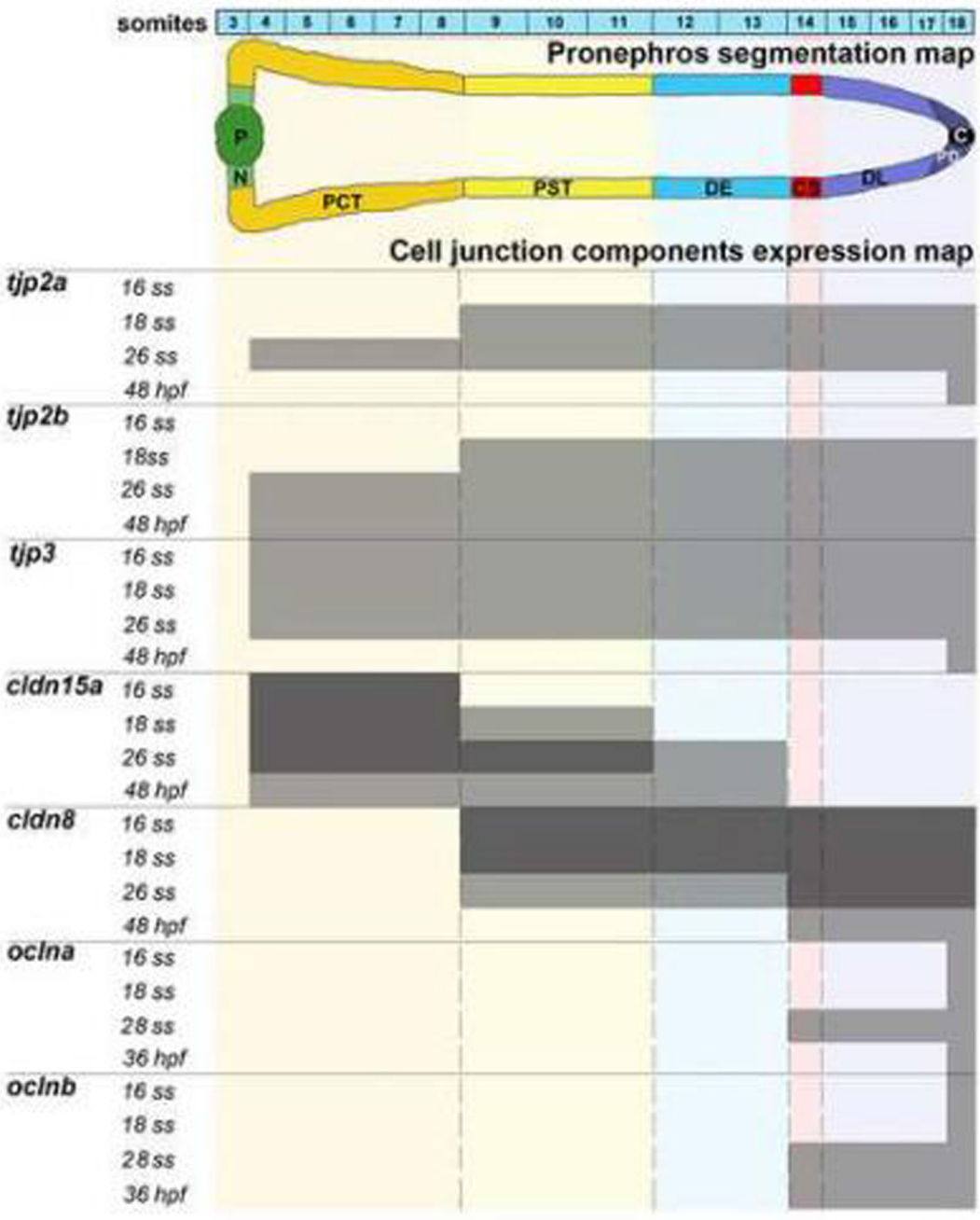

Figure 6. Spatiotemporal map of tight junction expression domains in the developing zebrafish pronephros

(Top) Nephron segment map of the pronephros. Segment identities form adjacent to particular somites (demarcated by numbered columns). Gene expression domains (black bars demarcate high expression and gray bars demarcate low/weak expression) are schematized in the pronephros territory between the 16 somite stage (ss) and 48 hours post fertilization (hpf). (Background) Each segment region is uniquely color-coded to compare gene expression domains at each time point with the nephron segment that forms at that

location. Segment color codes are as follows: PCT-orange, PST-yellow, DE-light blue, CS-red, DL-PD-dark blue.